

Electronic Supplementary Information

**Microgel-like aggregates of isotactic and atactic
poly(methacrylic acid) chains in aqueous alkali chloride solutions as
evidenced by light scattering**

Simona Sitar¹ Vladimir Aseyev,² and Ksenija Kogej^{1}*

¹ Department of Chemistry and Biochemistry, Faculty of Chemistry and Chemical Technology,
University of Ljubljana, P.O. Box 537, SI-1000, Ljubljana, Slovenia

² Laboratory of Polymer Chemistry, Department of Chemistry, University of Helsinki, P.O. Box
55, FIN-00014 HU, Helsinki, Finland

Experimental

Materials. The tacticities of both PMA samples were determined from their ester forms. For this purpose, the acids were dissolved in a methanol/water mixture (2:1) and an ethereal diazomethane solution was added while stirring to yield the methyl esters of polyacids, i.e. the poly(methyl methacrylates), PMMAs. The tacticities of the resulting PMMAs were determined from the signals of the α -methyl group in the ^1H NMR spectrum of a CDCl_3 solution as reported previously.¹ The results are reported in Table S1.

Table S1 Tacticities of PMA samples

	% of isotactic triads	% of syndiotactic triads	% of atactic triads
aPMA	3	69	28
iPMA-	93	3	4

Preparation of Solutions. aPMA is soluble in water at any α_N , whereas iPMA is soluble only if a portion of COOH groups are ionized. The critical value of α_N , denoted as $\alpha_{N,\text{crit}}$, at which iPMA dissolves in water at 25°C is $\alpha_{N,\text{crit}} \approx 0.2$.^{2,3,4} Different procedures were therefore used to prepare aPMA and iPMA solutions with various α_N values.

The stock solution of aPMA ($\alpha_N = 0$) was prepared by dissolving dry polymer (acid form) in 0.1 M XCl. After one day of stirring, when the polymer was visually dissolved, the solution was filtered through hydrophilic Sartorius-Minisart filters with a diameter 28 mm and pore size 0.45 μm . The concentration of the filtered aPMA solution was determined by potentiometric titration with a standardized aqueous 0.1 M NaOH solution. Solutions with higher α_N values ($\alpha_N = 0.25, 0.50, 0.75,$ and 1) were prepared by adding a calculated amount of 1 M XOH to the aPMA solution with $\alpha_N = 0$.

In the iPMA case, a stock solution with $\alpha_N \sim 0.5$ was used as the starting point to prepare solutions with other α_N values. The polymer was weighed and suspended in an appropriate amount of water. A calculated amount of 1 M XOH was slowly added to achieve $\alpha_N \sim 0.5$. The solution was stirred for ~ 2 days, with intermediate heating to around 50 °C for a few hours, and then filtered through 0.45 μm Sartorius filter. The exact α_N and c_p of this stock solution were determined after filtration by potentiometric titration with NaOH (the unionized COOH groups) and HCl (the ionized COOH groups). Solutions with other α_N values were prepared by adding a calculated amount of either 1 M XOH (for $\alpha_N > 0.5$) or 1 M HCl solution (for $\alpha_N < 0.5$). In the case of HCl addition, salt (XCl) that appeared in solution as a result of the protonation reaction was removed by dialysis against triple distilled water. After dialysis, these solutions were once again analyzed for concentration. The lowest α_N value studied in the iPMA case was chosen somewhat above $\alpha_{N,\text{crit}}$, i.e. at $\alpha_N \approx 0.25$, in order to assure that the polymer was completely dissolved. After all these procedures, the concentration of XCl in stock solutions was set to 0.1 M

by adding a more concentrated XCl solution of known concentration. Dilutions were done with the corresponding 0.1 M XCl. The majority of LS studies were performed in solutions with polymer concentration, c_p , equal to 0.023 M (where M denotes moles of carboxyl groups per volume). This concentration corresponds to 2 g/L at $\alpha_N = 0$. The concentration dependency was followed only for the 0.1 M NaCl case.

Light Scattering. Methodological aspects of dynamic, DLS, and static, SLS, light scattering can be found elsewhere.^{5,6} Detailed aspects of data analysis used in this paper are presented here.

LS experiments were conducted using the 3D cross-correlation spectrometer from LS Instruments GmbH (Fribourg, Switzerland), which is based on the 3D technology to filter single scattered light from the scattering signal;⁷ in this way, contributions of multiple scattering are dismissed. The instrument is suitable for particle characterization even in case of very turbid samples. Two coherent incident light beams are generated with a 20 mV He-Ne laser (Uniphase JDL 1145P), operating at a wavelength $\lambda_o = 632.8$ nm, and focused into the sample. The instrument is equipped with a laser attenuation system combined with an online incident laser intensity measurement that allows for the normalization of the LS data. Measurements were performed in cylindrical quartz sample cells. Solutions were gently filtered directly into the measuring cell through hydrophilic Millex-HV filters with a pore size of 0.22 μm and diameter of 13 mm. The initial few μL of the filtered solution were discarded. No significant loss of the polymer was observed due to filtering, which was verified by checking the intensity of scattered light from unfiltered and from filtered solution. The samples were allowed to equilibrate for 20 min before the measurement was initiated. Constant intensity of the light scattered at an angle of 90° was used as a criterion for proper equilibration. Intensity of scattered light was collected in the angular range from 40° and 150° . All LS studies were performed in solutions with $c_p = 2$ g L^{-1} and at 25°C .

Correlation functions of intensity of scattered light, $G_2(t)$, were recorded at an angle θ simultaneously with the integral time averaged intensities, $I_\theta \equiv I_q$, where $q = (4\pi n_o/\lambda_o)\sin(\theta/2)$ is the scattering vector and n_o is the refractive index of the medium. Intensities measured in counts of photons per second (cps) were normalized with respect to the Rayleigh ratio of toluene thus converting the cps-units into absolute intensity units given in cm^{-1} .

In order to determine the radius of gyration, R_g , of particles, two approaches were used: (i) for small particles (with sizes that fulfill the criterion $qR_g < 1$) the Zimm function was employed and (ii) for larger particles the Debye-Bueche scattering function was found to be the most suitable for R_g determination.^{5,6}

In order to determine hydrodynamic radii of particles, $G_2(t)$ was converted into the correlation function of the scattered electric field, $g_1(t)$, by using the Siegert's relationship.^{5,6} For monodisperse particles small in diameter compared to the wavelength of incident light as well as for hard spheres of any size, the relaxation time, τ , of the $g_1(t)$ function ($g_1(t) = \exp(-t/\tau)$) is related to the corresponding relaxation rate, $\Gamma = \tau^{-1}$, and the translational diffusion coefficient, D , by the relationship

$$g_1(t) = e^{-t/\tau} = e^{-\Gamma t} = e^{-Dq^2 t} \quad (1)$$

The hydrodynamic radius of particles, R_h , is then obtained from D via the Stokes-Einstein equation

$$R_h = \frac{kT}{6\pi\eta_0 D} \quad (2)$$

where k is the Boltzmann constant, T the absolute temperature, and η_0 the solvent viscosity.

For polydisperse samples, equation 1 can be written as a weighted average of all possible decays associated with several exponents (multiexponential function). For studied herein particles with moderately broad monomodal and bimodal size distributions, a bi-exponential or a multi-exponential fit to $g_1(t)$ was used. The bi-exponential fit was performed with ORIGIN 8.0 and the multi-exponential fit was based on the original inverse Laplace transform program CONTIN developed by Provencher.⁸ We collected 5-10 intensity correlation functions and averaged them. Each curve was analysed independently and compared with the averaged curve to ensure accuracy of the mathematical solution. Mean peak values of the size distributions, obtained at a fixed q and c_p , were used to estimate the apparent hydrodynamic radius, R_h^{app} . The R_h was then obtained by extrapolating R_h^{app} to $\theta = 0$. For data analysis, the relaxation times and rates were calculated from R_h .

The multi-exponential CONTIN fit was applied for the treatment of all correlation functions in aPMA solutions. In the iPMA case, however, at $\alpha_N > 0.25$, two relaxation times were too close to each other and the CONTIN analysis was difficult; the bi-exponential fit was used instead. Examples of data analysis are shown in Figs. S1 and S2.

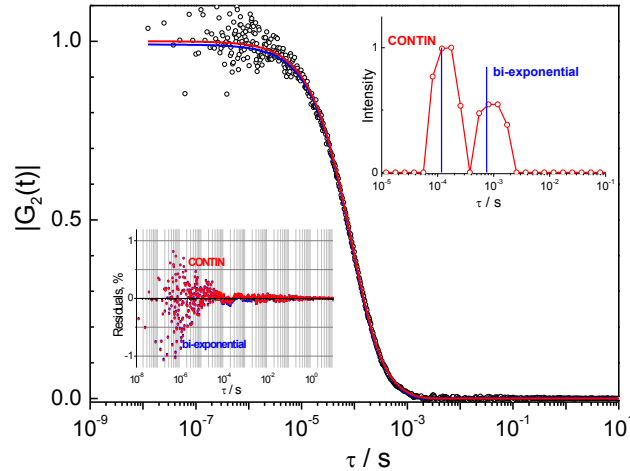


Fig. S1 Comparison of analysis of the correlation function made by CONTIN (red) and by bi-exponential fit (blue) for iPMA in 0.1 LiCl at $\alpha_N = 0.4$. The open black circles are experimental data. The upper inset represents relaxation time distributions of the corresponding $g_1(t)$ function, and the lower inset the residual error.

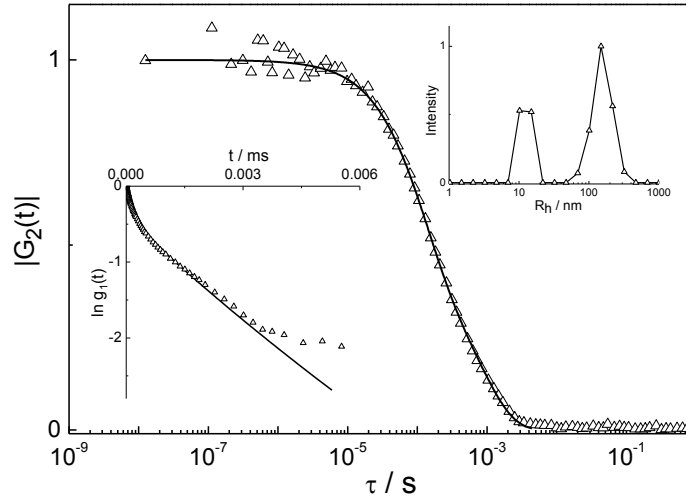


Fig. S2 Analysis of the intensity correlation function, $G_2(q,t)$, and the corresponding correlation function of the electric field $g_1(q,t)$, plotted as $\ln[g_1(q,t)]$ vs. t . Data obtained for aPMA sample in 0.1 M NaCl ($\alpha_n = 0.25$, $c_p = 2$ g/L) at a scattering angle of 90° . The dependence of $\ln[g_1(q,t)]$ on t represents two relaxation processes; consequently, the size distribution is bimodal.

In case of bimodal size distributions, each peak was treated separately to get two mean R_h values. Corresponding bimodal distributions of relaxation times were used to split the total intensity of scattered light into two relative contributions. Details of this procedure can be found elsewhere.^{9,10,11,12} The autocorrelation functions of scattered light intensity collected at a scattering vector q , $G_2(q,t) = \langle I(q,t=0)I(q,t) \rangle$, were recorded simultaneously with the integral intensities of scattered light, $I(q)$ (i.e. the total excess intensities of scattered light). The angular and concentration dependencies of $I(q)$ and the distributions of R_h , were analysed.

In case of bimodal size distributions of relaxation times, the calculated distributions were used to split total LS intensity into two contributions. Details of this procedure can be found elsewhere.^{9,10,11} For bimodal distributions with two well-separated peaks, each peak was treated separately. For each peak the mean peak values of τ_f (fast) and τ_s (slow) were calculated. Dependences of the corresponding relaxation rates Γ_f (or Γ_s) on the scattering vector q^2 are linear for aPMA and non-linear for iPMA and pass through the centre of coordinates (i.e. $\Gamma = 1/\tau = Dq^2$), thus representing a true diffusive process. The fast and the slow diffusing particles in the aPMA case are associated with individual chains (small particles) and intermolecular associates (large particles). In the iPMA case, the fast relaxation is assigned to aggregates of few chains (small particles) and to intermolecular associates (large particles).

In order to calculate the radii of gyration of the scattering particles, $R_{g,1}$ and $R_{g,2}$, we split the total LS intensity into two contribution using intensity weighted (also called unweighted) distribution of relaxation times τ (see Fig. S3). Each scattering species of the radius $R_{h,i}$ is represented in this distribution by its relative contribution, i.e. by the amplitude $A_i(\tau_i)$, to the total intensity of the scattered light $I(q)$. The relative amplitudes of the slow and fast relaxation processes have been estimated using the procedure outlined in works 9,10,11 as

$$A_f \equiv \sum_{fast} A_i(\tau_i) \quad \text{and} \quad A_s = 1 - A_f \quad (3)$$

Then we converted the relative amplitudes of the diffusive modes into the intensities of the light scattered by the particles of each type. The time-average intensities $I_f(q)$ and $I_s(q)$ were obtained as

$$I_f(q) = A_f(q) \cdot I(q) \quad \text{and} \quad I_s(q) = A_s(q) \cdot I(q) \quad (4)$$

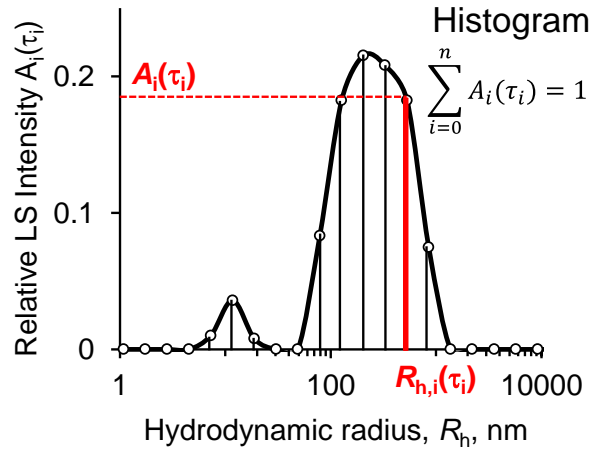


Fig. S3 Intensity weighted (or unweighted) distribution of hydrodynamic radii, R_h , or a histogram: the X-axis is a linear dependence of the relaxation time, τ , and the Y-axis shows relative contributions to the LS intensity, $A_i(\tau_i)$, scattered by a particle of the size $R_{h,i}$.

Results

Examples of the normalized correlation functions for iPMA and aPMA solutions in the presence of 0.1 M NaCl for all investigated α_N values are plotted in Figs. S4 and some additional decay rates as a function of q^2 for the slow mode in iPMA case with $\alpha_N = 1$ are shown in Fig. S5.

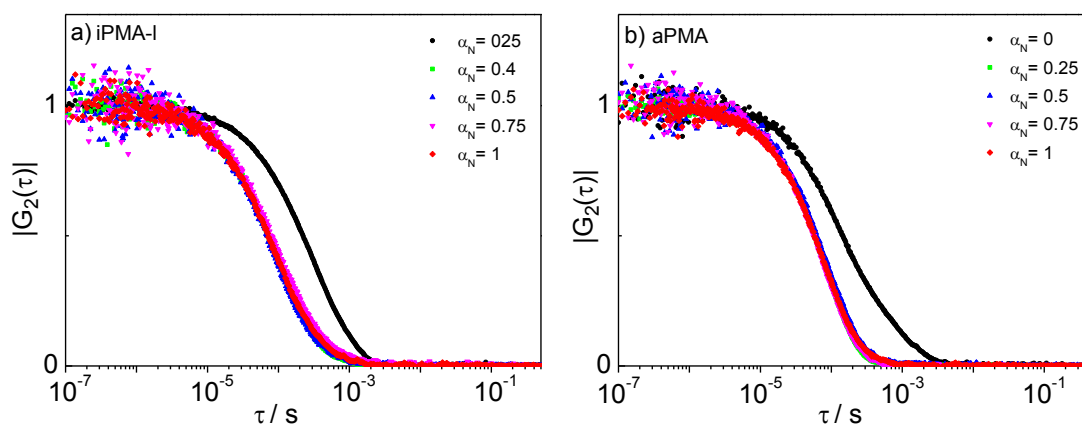


Fig. S4 Normalized intensity correlation functions for samples with different degrees of neutralization, α_N , at $\theta = 90^\circ$ for a) iPMA and b) aPMA.

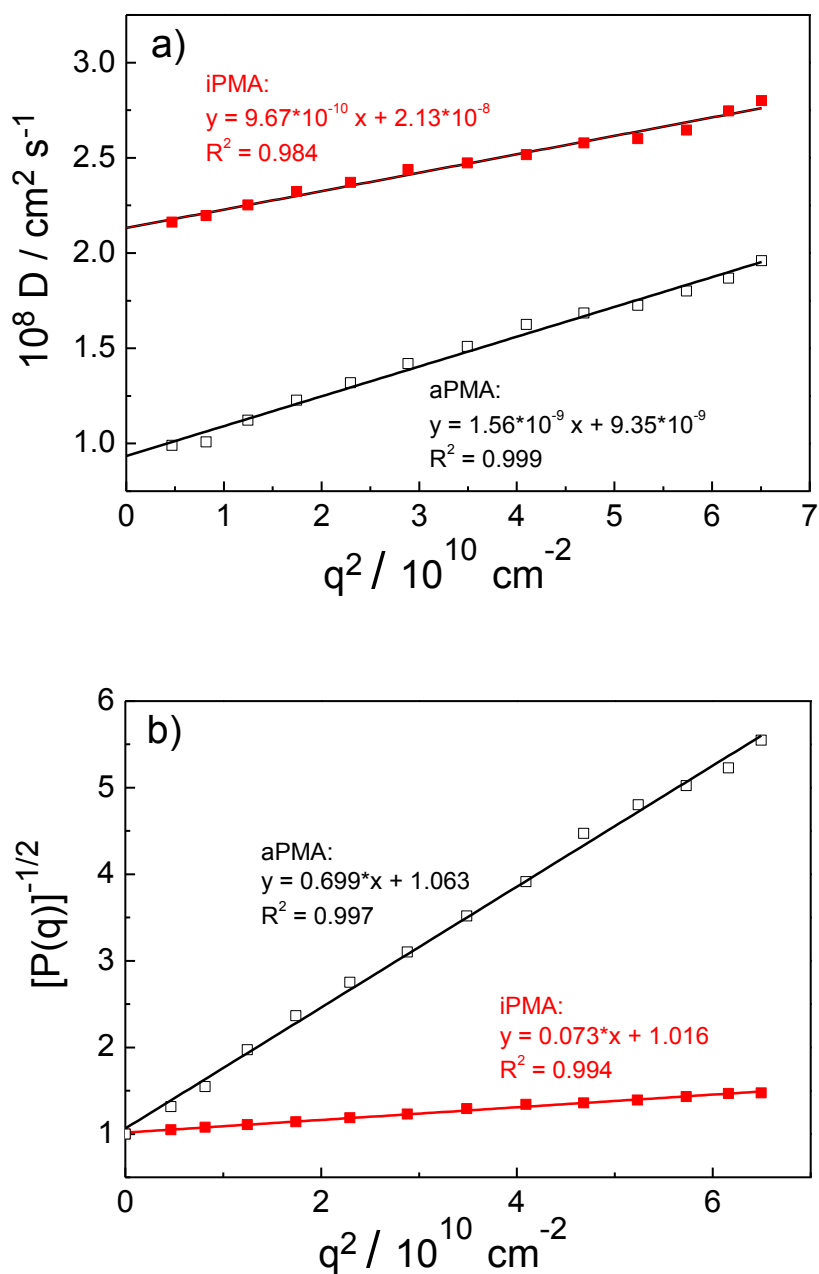


Fig. S5 Examples of LS data fitting for the determination of a) D (at $\theta = 0^\circ$) and b) R_g values of the aggregates in iPMA ($\alpha_N = 0.25$) and aPMA solutions ($\alpha_N = 0$) in 0.1 M LiCl. The upper plane: extrapolation of D to $\theta = 0^\circ$. The lower planes: the fit to the Debye-Bueche scattering function (represented as $1/\sqrt{P(\theta)}$ vs. q^2).

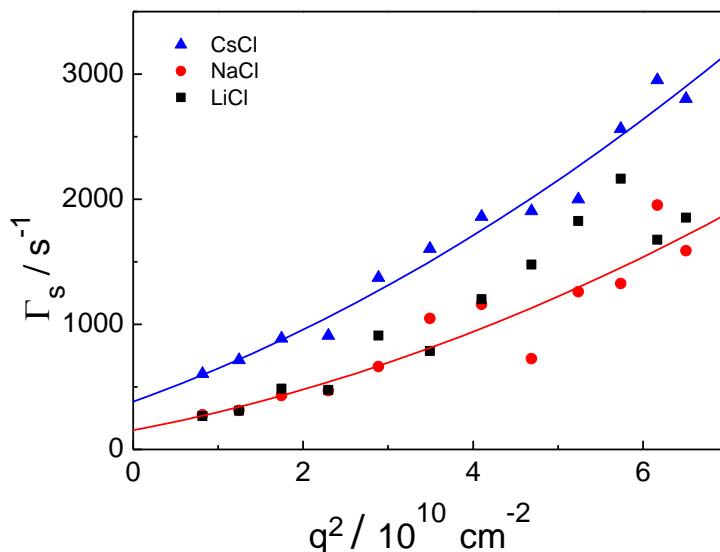


Fig. S6 Decay rates, $\Gamma = \tau^{-1}$, as a function of the square of the scattering vector, q^2 , at $\alpha_N = 1$ for iPMA in 0.1 M LiCl, NaCl, and CsCl and for aPMA in 0.1 M NaCl: only slow mode, Γ_s .

References

1. K. Kogej, H. Berghmans, H. Reynaers and S. Paoletti, *J. Phys. Chem. B*, 2004, **108**, 18164-18173.
2. N. Vlachy, J. Dolenc, B. Jerman and K. Kogej, *J. Phys. Chem B*, 2006, **110**, 9061-9071.
3. E. van den Bosch, Q. Keil, G. Filipcsei, H. Berghmans and H. Raynaers, *Macromolecules*, 2004, **37**, 9673-9675.
4. E. M. Loebl and J. J. O'Niell, *J. Polym. Sci.*, 1960, **45**, 538-540.
5. W. Schärfl, *Light Scattering from Polymer Solutions and Nanoparticle Dispersions*, Springer Verlag: Berlin, Heidelberg, 2007.
6. W. Brown, *Dynamic Light Scattering: The Method and Some Application*, Clarendon Press: Oxford, 1993.
7. C. Urban and P. Schurtenberger, *J. Colloid Interface Sci.* 1998, **207**, 150-158.
8. <http://s-provencher.com/index.shtml> (accessed Jan 26, 2011).
9. R. K. Klucker, J. P. Munch and F. Schosseler, *Macromolecules* 1997, **30**, 3839-3848.
10. E. Raspaud, D. Lairez and M. Adam, *Macromolecules* 1994, **27**, 2956-2964.
11. E. V. Tarassova, V. Aseyev, A. Filippov and H. Tenhu, *Polymer* 2007, **48**, 4503-4510.
12. M. Kanao, Y. Matsuda and T. Sato, *Macromolecules* 2003, **36**, 2093-2102.